Morphology and rheological behaviour of mixtures of poly(styrene-*b*-ethylene-*co*-butylene-styrene) block copolymer and poly(2,6-dimethyl-1,4-phenylene ether)*

Jin Kon Kim† and Dae Sung Jung
Research and Development Centre, Petrochemicals and Polymers, Lucky Limited, PO Box 10, Science Town, Daejeon 305-343, Korea

and Jinhwan Kim
Department of Polymer Science and Engineering, Sung Kyun Kwan University, Suwon 440-746, Korea
(Received 28 September 1992; revised 17 February 1993)

The morphology and rheological behaviour of binary mixtures of poly(styrene-*b*-ethylene-*co*-butylene-styrene) (SEBS) block copolymer (Kraton G1651) and poly(2,6-dimethyl-1,4-phenylene ether) (PPE), prepared by melt blending using a twin-screw extruder, were investigated. It was found that the cylindrical microdomains of the PS phase in Kraton G1651 were changed into lamellar microdomains in a mixture containing 14.3 wt% PPE. However, when the amount of PPE in a mixture was greater than 28 wt%, we found that part of the PPE was solubilized into the PS block of the copolymer, and the rest underwent macrophase separation. For a Kraton G1651/PPE mixture containing 28.6 wt% PPE, the microdomain structure in a melt blended sample was different from that found in a sample prepared by solution casting followed by annealing, although macrophase-separated PPE regions were observed in both samples. This observation led us to conclude that the morphology of mixtures of block copolymers and homopolymers depended upon the sample preparation method. In addition, it was found that plots of the dynamic shear modulus *versus* the loss modulus for these mixtures was a very useful method of monitoring the morphological change in mixtures of block copolymers and homopolymers as a function of composition or temperature.

(Keywords: SEBS/PPE mixtures; morphology; rheological behaviour)

INTRODUCTION

The phase behaviour of mixtures of block copolymers and homopolymers has been studied quite extensively[1-18]. Since block copolymers, such as poly(styrene-*b*-butadiene-styrene) (SBS), poly(styrene-*b*-isoprene-styrene) (SIS), and poly(styrene-*b*-ethylene-*co*-butylene-styrene) (SEBS), have microdomains, the morphology of block copolymer/homopolymer mixtures can be quite different from that of mixtures consisting of two homopolymers. In mixtures consisting of a block copolymer and a homopolymer, we observe two types of separation: (i) microphase separation where the domain size is of order of tens of nanometres, and (ii) macrophase separation in which the domain size is of order of micrometres[19]. It is now well established that the microdomain structure in block copolymer/homopolymer mixtures changes in a much more complicated fashion than does the microdomain structure of neat block copolymers, as a result of the two types of phase separation (i.e., microphase and macrophase separations) that occur in the former case[12,19].

Recently, Paul and co-workers[9-11] published a series of papers which dealt with the morphology and phase behaviour of mixtures of SEBS and PPE. They chose this system since the enthalpic force between the PPE and the PS block in the SEBS copolymer must be considered in addition to the entropic force, when determining phase transition behaviour. Hashimoto *et al.*[12] studied the morphological changes in mixtures of poly(styrene-*b*-isoprene) (SI) block copolymer and PPE, by varying the rate of solvent evaporation during the sample preparation. Specifically, they found that macrophase separation occurred in samples prepared by slow evaporation of solvent, while in samples prepared by fast evaporation of solvent only microphase separation was observed.

Some research groups[20-24] have studied the effect of a block copolymer on compatibilizing immiscible polymer blends. Other groups[25-27] have investigated the phase behaviour of block copolymer/homopolymer mixtures, in which the chemical structure of the homopolymer is identical to (or different from) one of the constituents in the block copolymer. To date, almost all of the studies reported in the literature[1-18] have dealt with samples prepared by solution casting, followed by annealing, in order to obtain an equilibrium morphology. It should be noted that theories[25-31] predicting the order–disorder transition temperature and the phase

* Presented in part at the 34th IUPAC International Symposium, July 1992, Prague, Czechoslovakia
† To whom correspondence should be addressed

0032-3861/93/224613-12

behaviour of these mixtures are also based on a thermodynamic equilibrium.

Commercial blends (or alloys) containing a block copolymer and two homopolymers, where the block copolymer plays the role of a compatibilizer, or impact modifier, are available[32]. Almost all of these commercial blends are prepared by an extrusion technique. In such processes, in addition to the thermodynamic miscibility between the block copolymer and the homopolymers the extent of shear applied and the viscosities of each component control the phase behaviour and the resulting morphology which, in turns, affects the final mechanical properties.

In this study, instead of using solution casting, we have used an extrusion method, which utilizes a twin screw extruder, to prepare blends of SEBS and PPE, and investigated the morphology and rheological behaviour of the mixtures obtained in this way.

EXPERIMENTAL

Materials

The PPE employed in these studies was a commercial grade material which was obtained from the Japan Polyether Co. Ltd. (Grade H-51). Its intrinsic viscosity, measured in chloroform at 25°C, was 0.515 dl g^{-1}. The weight-average molecular weight (M_w) and the second virial coefficient (A_2) of the PPE were 35 700 g mol^{-1} and 1.46×10^{-3} cm^3 mol g^{-2}, respectively, as determined by a low-angle laser light scattering (l.a.l.l.s.) technique, with chloroform as the solvent (at 25°C). The polydispersity index, M_w/M_n, determined by gel permeation chromatography (g.p.c.) using a polystyrene standard was 2.23.

The SEBS copolymer employed in this work was a commercial grade material (Kraton G1651) which was obtained from the Shell Development Co. The M_w of the entire block, determined by l.a.l.l.s., was found to be 174 000. Using ^1H and ^{13}C n.m.r. spectroscopy, the weight fraction of the PS block was found to be 0.33, giving the sequence of block molecular weights as 29 000(S)–116 000(EB)–29 000(S). In addition, the butylene (or 1,2 addition) portion of the soft block, i.e. poly(ethylene-*co*-butylene), was found to be 37.0 wt%. The polydispersity index of Kraton G1651, determined by g.p.c. using a polystyrene standard, was 1.09.

Blends of Kraton G1651/PPE were prepared by using a Leistritz intermeshing corotating twin extruder (model LSM 30.34GL: $l/d = 37.3$; 200 rev min^{-1}), while maintaining the barrel temperature at 290–300°C, with a residence time of ~2 min. The pellets obtained by the extrusion process were compression moulded at 280–290°C for 15 min. Neat Kraton G1651 and PPE were moulded as received. PPE was found to be very difficult to pelletize by extrusion at 300°C on account of its high viscosity. Therefore, we used compression moulding, in this case, in order to maintain the same thermal history for all of the blend samples. It should be noted that neat PPE could not be injection moulded due to its high viscosity. Values of the weight fractions of PPE in each blend prepared in this way are given in *Table 1*.

Table 1 Blend compositions of the SEBS/PPE system

Blend	PPE/SEBS (wt/wt)	PS/(PPE+PS) (%)	(PS+PPE)/(PPE+SEBS) (%)
P-1	14.3/85.7	67	43
P-2	28.6/71.4	45	52
P-3	42.9/57.1	31	62
P-4	57/43	20	71
P-5	71.5/28.5	13	81
P-6	85.7/14.3	5.3	90

Differential scanning calorimetry (d.s.c.)

Glass transition temperatures (T_gs) of the hard segments (i.e. PPE and the PS block in Kraton G1651) for all of the mixtures were measured using a differential scanning calorimeter (Perkin-Elmer DSC-7). Prior to the measurements, a baseline correction was obtained using two empty pans as a reference. In order to prevent thermal degradation, nitrogen gas was circulated through the sample chamber. Samples (~15 mg) were first heated to 250°C using a heating rate of 20°C min^{-1}, annealed for 3 min, and then quenched to room temperature at a cooling rate of 200°C min^{-1}. A second heating run was used to determine the T_gs of the specimens, which were read from the thermograms at the midpoints of the changes in the heat flow.

Dynamic mechanical thermal analysis (d.m.t.a.)

The storage modulus (E') and the loss tangent ($\tan\delta$) were measured using a dynamic mechanical thermal analyser (Polymer Laboratories), employing a single cantilever at a frequency of 1 Hz, and a heating rate of 3°C min^{-1}. For all of the blends, as well as neat Kraton G1651 and PPE, the temperature where $\tan\delta$ shows a maximum was taken as the T_g.

Rheological measurements

The dynamic shear modulus, $G'(\omega)$, and the loss modulus, $G''(\omega)$, at various angular frequencies, ω, were measured at 300°C by a Rheometrics mechanical spectrometer (RMS-800), using 25 mm circular discs. The shear viscosities, $\eta(\dot{\gamma})$, were obtained by using a capillary rheometer (Instron Model 3211) at 320°C.

Morphology

The morphology of the Kraton G1651/PPE blends was examined by using a transmission electron microscope (JEOL-100 CX). Specimens were cut, at approximately −120°C using a LKB ultramicrotome, and stained with ruthenium tetroxide (RuO_4) for 8 min (to improve contrast).

Mechanical properties

The tensile and flexural strengths were measured using universal test machines (Instron Model 4204, and Zwick Model 1425, respectively).

RESULTS AND DISCUSSION

Glass transition temperature and compatibility

In order to investigate the compatibility (or miscibility) between the PS block in Kraton G1651 and PPE, we obtained the d.s.c. thermograms at temperatures above ambient. The T_g of the soft segment, i.e. the EB block in Kraton G1651, in the blends was measured by d.m.t.a. and will be discussed later. The d.s.c. thermograms of all of the blends examined are given in *Figure 1*, where we observe that the transition takes place over a very broad temperature range (>100°C) in samples (P-1)–(P-5). In contrast, for sample (P-6), which has the largest PPE

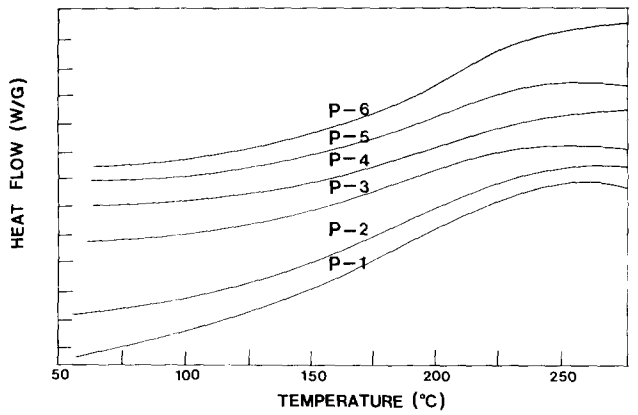

Figure 1 D.s.c. thermograms covering the transition regions of the hard segments in the Kraton G1651/PPE blends (compositions as shown in *Table 1*)

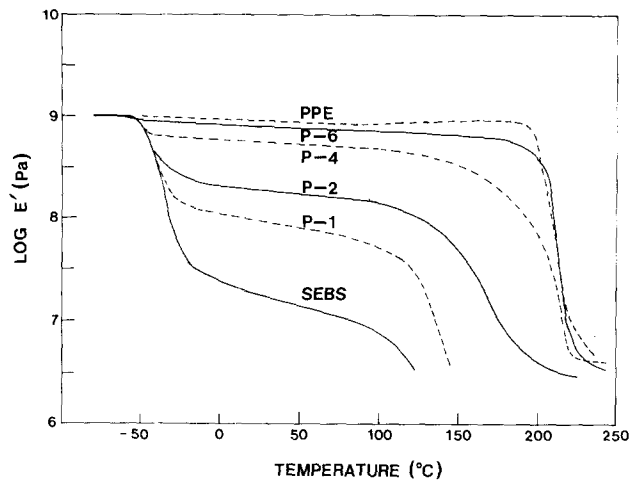

Figure 2 Elastic modulus (E') as a function of temperature for the Kraton G1651/PPE blends (compositions as shown in *Table 1*)

content of all of the various blends employed in this study, the transition takes place over a relatively narrow temperature range. One might be tempted to conclude from these results that all of the blends are compatible since a single value of T_g appears for each blend composition. However, such a conclusion should not be made in haste, since the range of the transition temperature, ΔT_g, i.e. the temperature difference between the final and the onset points, is very broad. Since the large values of ΔT_g observed in the Kraton G1651/PPE blends can be related to local inhomogeneities, such as local concentration fluctuations, we cannot exclude the possibility of the existence of two phases or micro-heterogeneity which cannot be detected by the d.s.c. measurements.

It should be mentioned here that Paul and co-workers[9-11] have also studied the ΔT_gs of SEBS/PPE blends. However, the values obtained by these workers are very small, when compared to those obtained in this study. It should be noted that the same SEBS block copolymer was used in both studies, and in addition the molecular weight of the PPE used in our work is almost identical to that used by Paul's group.

We therefore conclude that the very large range of T_g shown in *Figure 1* can be attributed to the extrusion process employed in the sample preparation (cf. the studies of Paul and co-workers[9-11] where solvent casting was used for sample preparation).

The elastic modulus (E') and loss tangent (tan δ) curves, for various blend compositions, are given in *Figures 2* and *3*, respectively. It can be seen from *Figure 2* that E' in the plateau region which appears at temperatures between -20 and 100°C increases gradually as the amount of PPE is increased, indicating that the PPE is solubilized into the PS block of the copolymer. It should be noted that at 25°C the value of E' of sample (P-1) is about an order of magnitude higher than that of Kraton G1651, which suggests that the microdomain structure of sample (P-1) is quite different from that of the neat copolymer.

Figure 3 shows that sample (P-1) has a single T_g, which appears at 140°C, i.e. between the T_g of the PS block in Kraton G1651 and the T_g of PPE; this suggests that the entire amount of PPE is solubilized into the PS block of the copolymer. This blend was transparent when observed visually, and no delamination took place when a moulded specimen was fractured. This complete solubilization of PPE into the PS block of Kraton G1651 can be tested by comparing the measured T_g of the blend with the value of T_g predicted by the Fox equation[33]:

$$1/T_g = w_{PS}/T_{g_{PS}} + w_{PPE}/T_{g_{PPE}} \quad (1)$$

where w_{PS} and w_{PPE} are the respective weight fractions of the PS block and the PPE in the total hard segments ($w_{PS} + w_{PPE} = 1$), and $T_{g_{PS}}$ and $T_{g_{PPE}}$ are the glass transition temperatures of the PS block in neat Kraton G1651, and PPE, respectively. We found that the values of $T_{g_{PS}}$ and $T_{g_{PPE}}$ as determined by d.m.t.a., were 110 and 215°C, respectively. Since w_{PPE} in the total hard segments of sample (P-1) is 0.33 (see *Table 1*), the value of T_g predicted by equation (1) is 139°C, which is very close to the value measured experimentally (140°C). For sample (P-2), *Figure 3* shows a single T_g at 165°C, but no peak is observed at close to 215°C, from which we can speculate that the entire amount of PPE is solubilized into the PS block of Kraton G1651. However, this blend was translucent in appearance, and delamination occurred when a moulded specimen was fractured. These observations led us to speculate that macrophase-separated domains of PPE may exist in this sample. It should be noted that the T_g of sample (P-2), i.e. 165°C, corresponds to the T_g of a blend in which 58 wt% of PPE

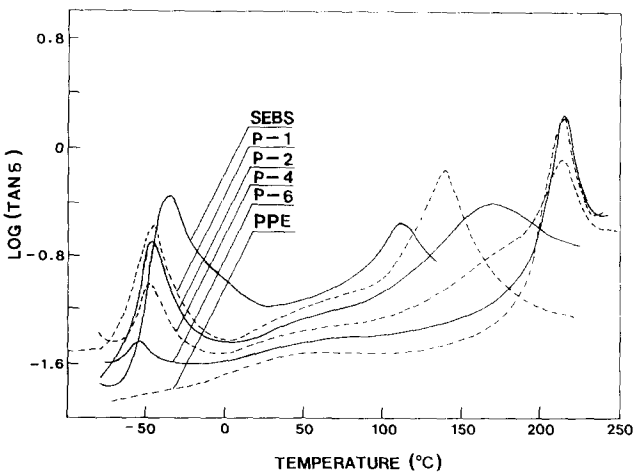

Figure 3 Loss tangent (tan δ) as a function of temperature for the Kraton G1651/PPE blends (compositions as shown in *Table 1*)

is solubilized completely in the PS block of Kraton G1651, if equation (1) is used. It should also be noted that in sample (P-2) the amount of PPE in the total hard segments was 55 wt% (see *Table 1*).

For sample (P-4), the T_g appearing at 215°C is essentially identical to the T_g of neat PPE, while a shoulder in the curve can be seen at ~165°C. Thus, it is reasonable to speculate that in this sample, part of the added PPE was solubilized into the PS block of Kraton G1651, with the largest portion of the added PPE existing as a macrophase-separated domain. For sample (P-6), which contains the highest content of PPE of all of the blend samples examined in this work, the shoulder that was observed in sample (P-4) is barely noticeable. It should be mentioned that for all of the blends studied here, no peak appears at or near 110°C, which is the T_g of the PS block in neat Kraton G1651. This means that *at least* part of the added PPE could have been solubilized into the PS block, until a limiting value was reached.

It is of interest to note that in *Figure 3* the temperature corresponding to the shoulder appearing in the tan δ curve (at ~165°C) for samples (P-4) and (P-6) is almost the same as the T_g of sample (P-2). As discussed above, 165°C corresponds to the T_g of a blend in which 58 wt% of added PPE is solubilized into the PS block of Kraton G1651. Thus, for samples (P-4) and (P-6), in which the amount of PPE in the total hard segments exceeds 58 wt%, this actual amount of PPE was solubilized into the PS block of Kraton G1651, while the rest has probably remained in the separate domains of the neat PPE. Therefore, we conclude that for samples (P-4) and (P-6) where two T_gs are detected by the d.m.t.a. measurements, one of these corresponds to the T_g of the PS domain in which part of the added PPE is solubilized, with the other corresponding to the T_g of the macrophase-separated domains of the PPE.

It should be mentioned that the T_g of a Kraton G1651/PPE mixture may depend on the sample preparation method that is employed. For example, Paul and co-workers[9–11] measured the T_gs of Kraton G1651/PPE blends that had been prepared by precipitation followed by compression moulding, and reported that a single T_g was observed for all blend compositions. It is reasonable to speculate that the extent of mixing between the PS block and PPE for samples prepared by twin screw extrusion using a very short residence time (~2 min), as used in this work, might not be as good as that in samples prepared by precipitation from solution.

Let us now consider the T_g of the soft segment, the EB block in Kraton G1651, which appears at approximately −40°C (see *Figure 3*). Using the peak positions of the tan δ curves the T_g of the EB block is plotted as a function of the composition, and is given in *Figure 4*. It is worth noting that in this figure the T_g of the EB block decreases as the amount of PPE is increased. Recently, Paul and co-workers[10] reported similar observations in SBS/PPE blends. In addition, Han *et al.*[13] have observed that the T_g of the PB block in a neat SBS block copolymer was higher than that measured for its blends with poly(α-methylstyrene) (PαMS) when the molecular weight of the latter was relatively high. It should be noted that in the blends employed by Paul and co-workers[10] and Han *et al.*[13] no macrophase-separated regions were present, while in some of the blends employed in this current study macrophase-separated regions did exist. Nonetheless, it has been observed in all of the systems

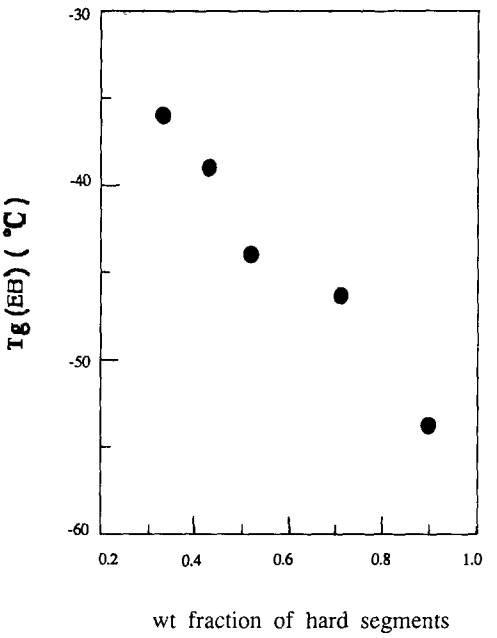

Figure 4 T_g of the EB block as a function of the weight fraction of the hard segments in the Kraton G1651/PPE blends. Values are taken from the lower-peak values in *Figure 3* (see text for details)

described above that the T_g of the soft segment in the block copolymer was shifted toward a lower temperature as the total fraction of the hard segments in the blends was increased.

In earlier work, Bohn[34,35] and Morbitzer *et al.*[36] found that in poly(acrylonitrile–butadiene–styrene) (ABS) terpolymer, the T_g of the rubber (PB) domains in the hard matrix of poly(styrene-*co*-acrylonitrile) (PSAN) was shifted toward a lower temperature as the weight fraction of the rubber in the ABS was decreased. Born[34,35] explained this behaviour as follows. With decreasing amounts of rubber phase, the difference in the thermal expansion coefficients between the rubber phase and the rigid matrix becomes larger, and causes the thermal stress (i.e. negative hydrostatic pressure) to increase around the rubber phase. Since this increased thermal stress becomes a source of the volume dilation of the rubber domain, the T_g of the latter decreases as the amount of rubber phase in the system is decreased. He also found that as the amount of rubber phase was reduced, the onset temperature of the glass transition ($T_{g,i}$) usually remained unchanged, while the final temperature of the glass transition ($T_{g,f}$) decreased. Thus a peak in the tan δ curve (i.e. T_g) of *Figure 3*, which appeared at about the midpoint between $T_{g,i}$ and $T_{g,f}$, was shifted toward a lower temperature with reduced amounts of rubber phase. Morbitzer *et al.*[36] further found that when the thermal stress resulting from the difference in thermal expansion coefficients overcame the adhesion between the rubber domain and the rigid matrix, the T_g of the rubber phase then increased with increasing rubber content. This led these authors to conclude that the adhesion between the rubber phase and the rigid matrix, in addition to the thermal stress resulting from differences in the thermal expansion coefficients, also plays an important role in determining the T_g of the rubber phase as a function of the rubber content in these ABS systems.

It should be mentioned that the above explanations are valid for blends where the rubber phase (or soft

segment) forms a dispersed phase in the rigid matrix of the hard segments. For block copolymers, where the soft segment forms the dispersed phase (or microdomain structure) in the matrix of the hard segments, the fact that the T_g of the soft segment was shifted toward a lower temperature with decreasing amounts of the soft segment[37] can be explained by using the same argument as presented above. It should be noted that for certain blend compositions employed in this study, as well as the SBS/PαMS blends studied by Han *et al.*[13], the microdomain structure of the hard segments was an alternating lameller type.

It is reasonable to state that for the blends employed in this study PPE could not possibly be solubilized into the EB block in Kraton G1651 due to the rather poor miscibility between these two components. If PPE were solubilized into the EB block of the copolymer, the T_g of the block should have increased with increasing amounts of PPE. As mentioned above, the microdomain structure in sample (P-1) is actually an alternating lamellar type, and this will be discussed further below. Therefore, the soft phase in the Kraton G1651/PPE blends employed in this study could not form the matrix phase.

Another possible explanation for the reduction in the T_g of the EB block of the copolymer in these blends as the amount of this block is decreased, is that the interfacial thickness between the EB block and the mixed phase of the PS block and PPE might become thinner with increased amounts of PPE. It should be noted that a reduced interfacial thickness may give rise to a lower T_g of the EB block in the mixture. In sample (P-1), for example, in which the entire amount of PPE is solubilized into the PS block, the interfacial thickness becomes smaller than that of Kraton G1651, if the interaction parameter between the PS block and the EB block is less than that between PPE and the EB block. However, as the amount of PPE in the mixtures was increased (e.g., in samples (P-2)–(P-6), where two phase structures were found), it is less likely that large changes in the interfacial thickness between the two components should occur. Therefore, the large shift in T_g of the EB block toward a lower temperature with increasing amounts of PPE (as shown in *Figure 4*) might not be satisfactorily explained by differences in interfacial thickness, but is most likely to result from the difference between the thermal expansion coefficients of the hard matrix and the soft domain structure.

Microdomain structure

Transmission electron micrographs of neat Kraton G1651 and Kraton G1651/PPE blends are given in *Figures 5* and *6*, respectively. The PS block and PPE are stained by RuO_4 and therefore the dark areas represent these components, while the white area represents the EB block. *Figure 5a* shows that Kraton G1651 has cylindrical microdomains which contain PS blocks. It should be noted that when a sample, which has a hexagonal (or cylindrical) microdomain structure, is cut parallel to the hexagonal axis, the structure appears to be lamellar[38], as shown in *Figure 5b*. Recently, using small-angle X-ray scattering (SAXS) and transmission electron microscopy (TEM) Sakurai *et al.*[39] found that: (i) the microdomain structure of a Kraton G1652 sample having a PS weight fraction of 0.286 and a 'total' molecular weight of 52 500, consisted of cylindrical microdomains of the PS block in the matrix of the EB block, if the sample was cast from *o*-dichlorobenzene at 140°C, and; (ii) this microdomain structure became lamellar when the sample was cast from toluene at room temperature. However, if annealed at 200°C, this lamellar morphology was destroyed and the sample once again showed cylindrical microdomains of PS blocks. These authors therefore concluded that the equilibrium morphology of Kraton G1652 was the cylindrical morphology. Although the weight fraction of the PS block in Kraton G1652 that was used by Sakurai *et al.*[39] is similar to that in Kraton G1651, the total molecular weight is only about one third of that of the latter copolymer. It is now well established that the morphology of a block copolymer is predominantly determined by the volume (or weight) ratio of the two blocks, and the total molecular weight does not play an important role in controlling the microdomain morphology, as long as it is larger than a certain critical value[38,40].

It can be seen from *Figure 6a* that the microdomain structure of sample (P-1) has the lamellar morphology, which led us to speculate that the entire amount of added PPE was solubilized into the PS block. This speculation seems quite reasonable as the total amount of hard segments in blend (P-1) is 43 wt% (see *Table 1*). We are of the opinion that in this present study lamellar structures were not perfectly developed due to the use of melt blending, instead of solution casting, as the method of preparation.

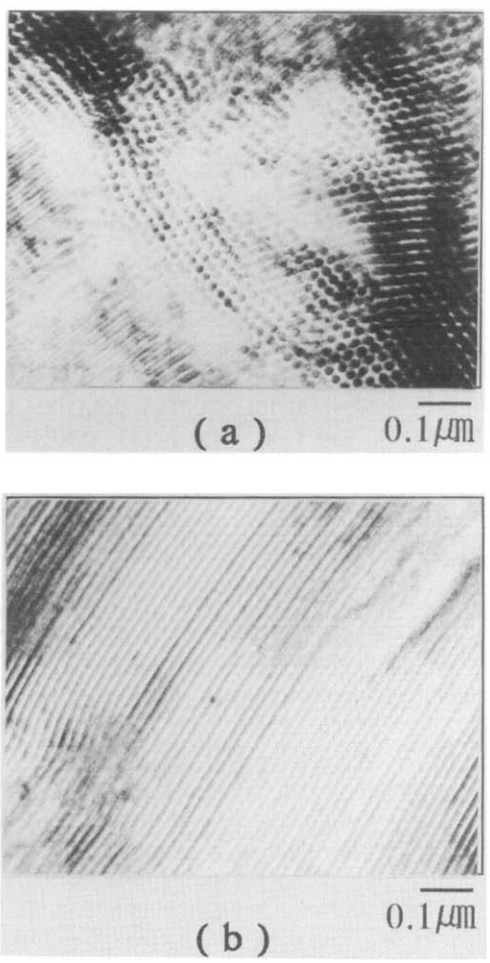

Figure 5 Transmission electron micrographs of Kraton G1651: a, perpendicular to the hexagonal axis and; b, parallel to the hexagonal axis

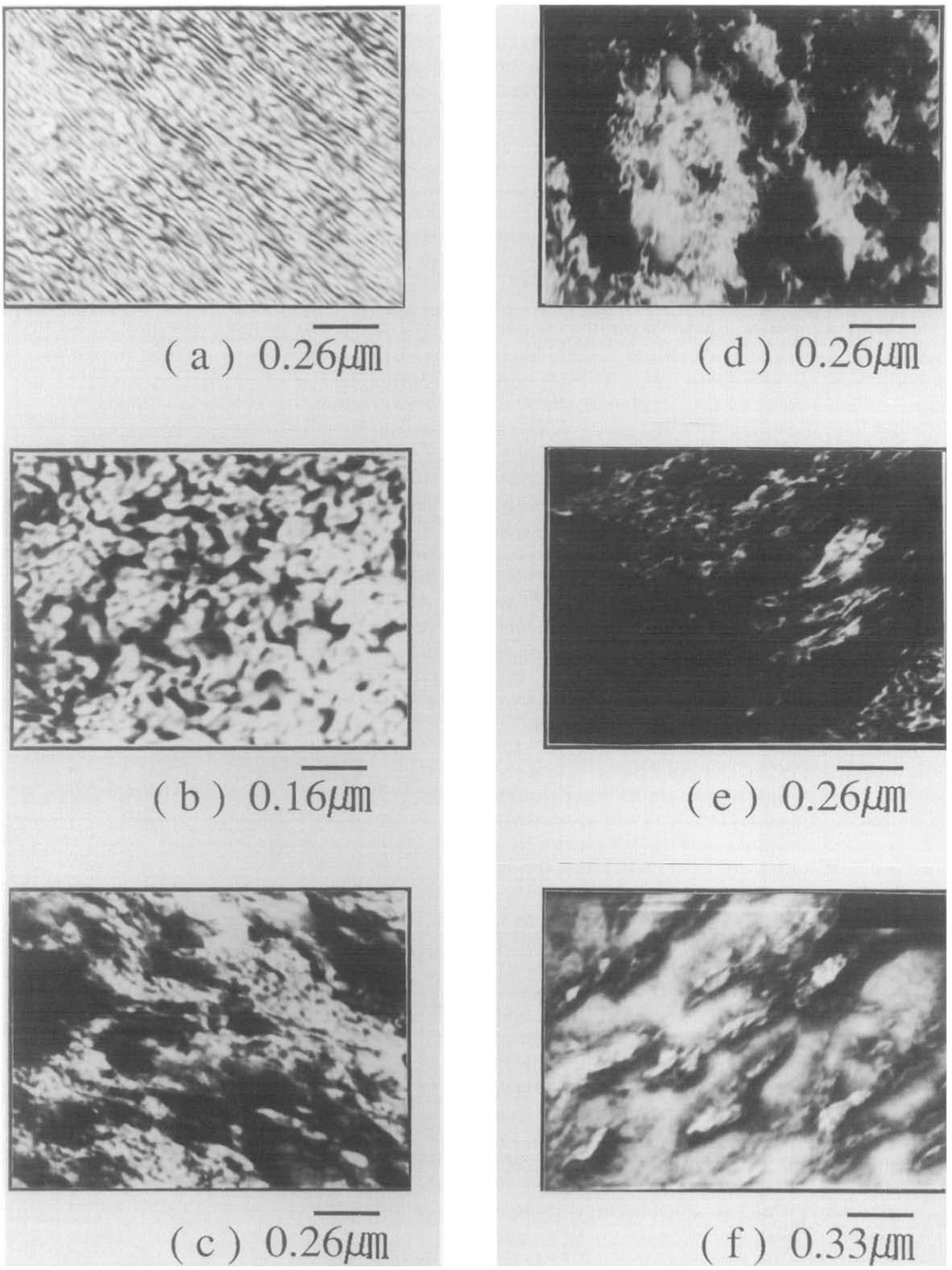

Figure 6 Transmission electron micrographs of Kraton G1651/PPE blends: a, (P-1); b, (P-2); c, (P-3); d, (P-4); e, (P-5); f, (P-6). The compositions of the blends are given in *Table 1*

It is of interest to note that in sample (P-2) (see *Figure 6b*), part of the PPE component (shown as the darker area) exists as macrophase-separated domains, while the morphology of the microphase shows a cylindrical or complex structure. It should be noted that Han *et al.*[13] reported similar observations for mixtures of a SBS block copolymer and PαMS. The experimental observations that blend (P-2) was translucent and showed delamination when a moulded specimen was fractured (see above), can be explained by the existence of macrophase-separated PPE, which is clearly seen in *Figure 6b* (see also *Figure 7*, which is a transmission electron micrograph of blend (P-2) which was obtained at a lower magnification). The question can then be asked as to why a single T_g is observed, by d.m.t.a. (or d.s.c.), for sample (P-2) (see *Figure 3*). This puzzling behaviour was also observed by Paul and co-workers[10] for blends of an SBS copolymer and PPE. In *Figures 6b* and *7*, since the PS block and the PPE were stained by RuO_4, the dark areas outside the block might be PPE domains

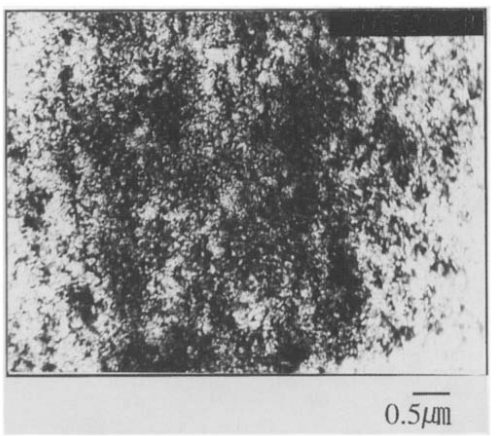

Figure 7 Transmission electron micrograph of blend (P-2), obtained at a lower magnification (cf. *Figure 6b*); composition given in *Table 1*

which were not solubilized into the former. We were not able to detect the T_g of the macrophase-separated PPE (~215°C) by using d.s.c. and d.m.t.a. This could perhaps be explained by the size of the phase-separated PPE domain, which could only be detected by TEM techniques. If the entire amount of added PPE was solubilized into the PS domain of Kraton G1651, sample (P-2) would have appeared transparent (c.f. sample (P-1)). However, this blend was translucent in appearance. It is worth mentioning here that d.s.c. can detect local inhomogeneities in sizes of $\geqslant 50$ nm, while d.m.t.a. can detect even smaller sizes. Therefore, it does seem that more sophisticated methods such as solid-state n.m.r. spectroscopy, must be employed in order to detect the domains that have sizes smaller than 50 nm.

It can be seen from *Figures 6c–f* that in samples (P-3) and (P-4) the domain structure seems to be co-continuous, with block copolymer and macrophase-separated PPE being observed (consistent with the d.m.t.a. data), while in samples (P-5) and (P-6), block copolymer exists as a separate domain in the matrix of the PPE.

It is of interest to note that the microdomain structure of the PS block in Kraton G1651 for all of the blends studied here, except for sample (P-1), appears to be cylindrical in nature. Many research groups[2,3,12,13] have reported that the microdomain structure of a block copolymer in its mixtures with a homopolymer can change with increasing amounts of the latter. For example, Hashimoto *et al.*[12] showed that for SI/PPE blends the initial lamellar microdomain structure in the neat SI was transformed into spherical microdomains of PI blocks in the matrix of the PS blocks in which added PPE has been solubilized, as the amount of PPE was increased. Also, Han *et al.*[13] reported that for SBS/PαMS blends the cylindrical microdomain structure of the PS block in the neat SBS changed to a lamellar form (a reversed structure was even reported) when a sufficient amount of PαMS was added. Note that for both of these blend systems all specimens were prepared by solution casting followed by annealing, in order to produce an equilibrium morphology.

In order to check whether or not the microdomain structure of the PS block in a Kraton G1651/PPE blend changed with increasing amounts of added PPE, we used a solution casting method to prepare blends having the same composition as sample (P-2), followed by annealing at 220°C. A transmission electron micrograph of this blend is given in *Figure 8a*, and shows clearly that the cylindrical microdomain structure of the PS block in Kraton G1651 has changed to a lamellar microdomain structure, although the macrophase-separated PPE phase is still observed. It should be mentioned that the total hard segment in this blend is about 52 wt% (see *Table 1*), which can develop a lamellar microstructure under equilibrium conditions. It should be noted that the microdomains in a sample of blend (P-2) which was prepared by extrusion, exhibited a cylindrical or complex structure, and macrophase separations of PPE were clearly observed (shown in *Figure 8b*).

The observations allow us to speculate that, with the exception of sample (P-1) both macrophase separation of PPE and microphase separation in the Kraton G1651 occurred when blend samples were prepared by extrusion. Note that the solubilized PPE and the PS block of Kraton G1651 did not have sufficient time to develop an equilibrium morphology, as a result of the short contact time and high order–disorder transition temperature of neat Kraton G1651, which will be discussed below. Therefore, it can be concluded that: (i) in sample (P-1), which has 14.3 wt% PPE, the entire amount of added PPE was solubilized into the PS domain; (ii) in sample (P-2) most of the PPE was solubilized into the PS domain, while the remainder stayed either at the interface between the Kraton G1651 and the PPE or in macrophase-separated PPE domains and; (iii) in mixtures containing larger amounts of PPE, such as samples (P-5) and (P-6), some of the PPE was solubilized into the PS domain of the block copolymer, but the majority existed in the macrophase-separated PPE domain.

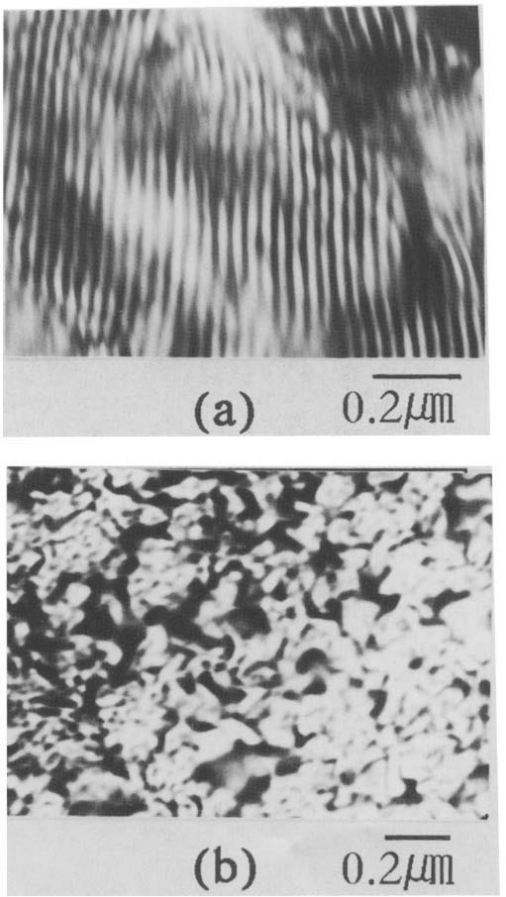

Figure 8 Transmission electron micrographs of blend (P-2) produced by: a, solution casting followed by annealing; b, melt blending. Composition is given in *Table 1*

Rheological behaviour of the blends

Logarithmic plots of the dynamic shear modulus (G') and the loss modulus (G''), both as a function of the angular frequency (ω), were obtained at 300°C, for all of the blends, including neat Kraton G1651 and PPE, and are given in *Figures 9* and *10*, respectively. It can be seen from these figures that at this temperature, Kraton G1651 behaves as a typical crosslinked material[41], showing only a slight variation in $G'(\omega)$ at lower values of ω. In samples (P-5) and (P-6), which contain large amounts of PPE, the rheological behaviour of the blends resembles that of typical thermoplastic materials. The dependence of both $G'(\omega)$ and $G''(\omega)$ on ω for Kraton G1651 at 300°C can be explained in part when we consider the order–disorder transition temperature (T_r) of a block copolymer from a theoretical point of view. At temperatures below T_r, a block copolymer, from rheological considerations, behaves as a 'filled' system or crosslinked material, while at temperatures above T_r, it behaves as a Newtonian fluid. Thus, from the rheological behaviour illustrated in *Figures 9* and *10*, the T_r of neat Kraton G1651 is believed to be much higher than 300°C. A theoretical prediction of the T_r of Kraton G1651 requires an exact expression for the Flory interaction parameter between PS and poly(ethylene-*co*-butylene) (PEB), χ_{PS-PEB}. Recently, Koberstein *et al.*[42] reported that the T_r of a SEBS block copolymer, which has a total molecular weight of 33 500 and a weight fraction for the PS block of 0.32, was 197°C. They also obtained an expression for

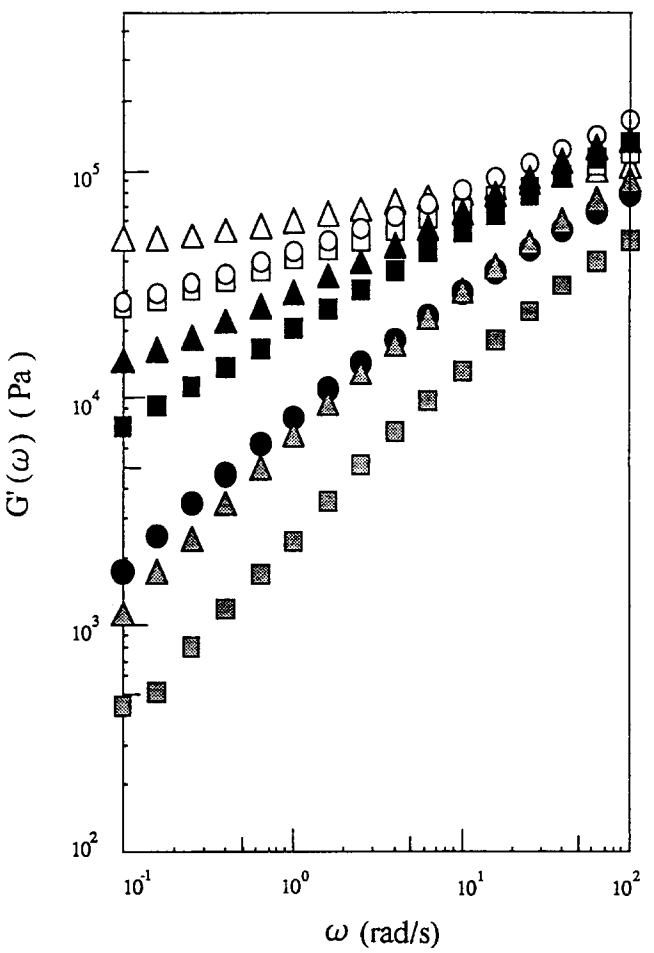

Figure 9 Log $G'(\omega)$ *versus* ω for the Kraton G1651/PPE blends at 300°C: △, Kraton G1651; ○, (P-1); □, (P-2); ▲, (P-3); ■, (P-4); ●, (P-5); ◬, (P-6); ▨, PPE. The compositions of the blends are given in *Table 1*

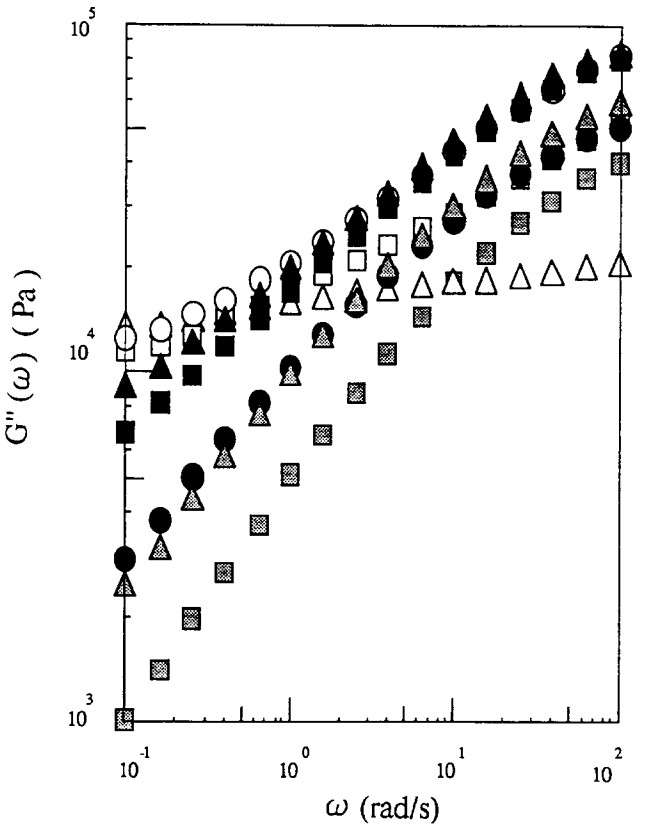

Figure 10 Log $G''(\omega)$ *versus* ω for the Kraton G1651/PPE blends at 300°C: △, Kraton G1651; ○, (P-1); □, (P-2); ▲, (P-3); ■, (P-4); ●, (P-5); ◬, (P-6); ▨, PPE. The compositions of the blends are given in *Table 1*

χ_{PS-PEB}, based on a random phase approximation, which was as follows:

$$\chi_{PS-PEB} = 0.0357 + 21/T \quad (2)$$

where T is the absolute temperature. As equation (2) was only based on SAXS measurements obtained at two temperatures, we still consider that more experiments must be carried out in order to obtain a more precise expression for χ_{PS-PEB}.

We have estimated the T_r of a poly(styrene-*b*-butadiene-styrene) (SBS) copolymer where the molecular weight of each block is the same as that of the Kraton G1651 employed in this study, since many different expressions for χ_{PS-PB} are available in the literature[43–46]. Here, we have used two different expressions for the interaction energy density, Λ_{PS-PB}. These are:

$$\Lambda_{PS-PB} = 1.573 - 0.0021T + 0.09\phi_{PS} \quad (3)$$

according to the work of Roe and co-workers[43,44], and:

$$\Lambda_{PS-PB} = 1.490 - 0.00179T \quad (4)$$

according to the work of Rounds[45]. It should be noted that Λ_{PS-PB} is given by:

$$\Lambda_{PS-PB} = (\chi_{PS-PB}/V_{ref})RT \quad (5)$$

where V_{ref} is the molar volume of a reference component (styrene), ϕ_{PS} is the volume fraction of PS in the SBS, copolymer, and R is the molar gas constant. The specific volume of PS was obtained from[47]:

$$v_{PS} = 0.9199 + 5.098 \times 10^{-4}(T-273) + 2.354 \times 10^{-4}(T-273)^2 + [32.46 + 0.1017(T-273)]/M_{w,PS} \quad (6)$$

where $M_{w,PS}$ is the molecular weight of the PS block, while the specific volume of PB was obtained from[48]:

$$v_{PB} = 1.1138 + 8.24 \times 10^{-4}(T - 273) \quad (7)$$

Before initiating the calculations of T_r, by using either the Helfand–Wasserman theory[49–51] or the Leibler theory[52], there are other quantities which have to be either given or defined. These are: (i) the Kuhn statistical lengths, b_k (where k = PS and PB), which are needed in the Helfand–Wasserman theory[49–51], (we have used $b_{PS} = 0.68$ nm and $b_{PB} = 0.69$ nm[53]) and; (ii) the polymerization index N in the Leibler theory[52]. In this work, we have calculated N using the following expression:

$$N = [M_{w,PS}v_{PS} + M_{w,PB}v_{PB}]/V_{ref} \quad (8)$$

For details of the computational procedures employed in obtaining the values of T_r (which are given in *Table 2*) interested readers are referred to the paper by Han *et al.*[54].

It can be seen from *Table 2* that the T_r of SBS based on both the Helfand–Wasserman and the Leibler theories is approximately 400°C or higher. According to Gergen[55], the solubility parameter difference between PS and PEB is about double that of the corresponding difference between PS and PB. Therefore, the miscibility between PS and PEB is believed to be much poorer than that between PS and PB, leading us to conclude that the T_r of the Kraton G1651 investigated in these studies would be even higher than the values given in *Table 2*. When equation (2) was used, we found that the predicted value of T_r of Kraton G1651 was greater than 500°C. Very recently, Kawamura *et al.*[56] reported that the T_r of a SEBS copolymer, which had a total molecular weight of 51 000 and a weight fraction of the PS block of 0.32, was ~290°C. It should be noted that since the total molecular weight of the SEBS copolymer used by Kawamura *et al.*[56] is about one third of that of Kraton G1651, the T_r of the latter would be much higher than 300°C.

Based on the theoretical prediction of the T_r of Kraton G1651, we speculate that the extrusion temperature of 300°C that was used in this work was far below the transition temperature of Kraton G1651, and that this was responsible for the poor contact of the PS block and PPE, as complete dissolution of the microdomain structure of the PS block in Kraton G1651 could not be attained at 300°C. It should be mentioned here that the predicted values of T_r given above are only valid for equilibrium-theory conditions. At present, there is no theory available which allows us to predict the T_r of a block copolymer under shear-flow conditions.

It can be seen from *Figure 9* that $G'(\omega)$ decreases steadily with increasing amounts of PPE. At lower ω values, the values of $G'(\omega)$ of sample (P-3) (or (P-4)) are about an order of magnitude larger than those of sample (P-5) (or (P-6)), leading us to conclude that a dramatic change in morphology between the two samples might take place, which is consistent with the TEM observations described above. It can be seen in *Figure 9* that the slope of the $\log G'(\omega)$ *versus* $\log \omega$ plot for neat PPE is less than two, since the PPE used here is a polydisperse polymer.

Using the results shown in *Figures 9* and *10*, $\log G'(\omega)$ *versus* $\log G''(\omega)$ curves were then plotted, and these are given in *Figure 11*. It is noted that these plots are very sensitive to the morphology of the respective blends[57]. It can be concluded from *Figure 11* that at 300°C the elasticity of Kraton G1651 is the largest, with values gradually decreasing as the amount of PPE is increased. It can also be seen that the plots obtained for samples (P-5) and (P-6) are very similar, which is consistent with the results obtained from the TEM investigations (see *Figures 6e* and *f*). It should be noted that in both of these samples Kraton G1651 is only present as a 'minor' phase in the matrix of the PPE.

A plot of the dynamic viscosity, $\eta'(\omega)(= G''(\omega)/\omega)$, of Kraton G1651 as a function of ω is given in *Figure 12* (along with corresponding plots for the various blends and also PPE) and shows highly non-Newtonian behaviour, which is further evidence that the T_r of the block copolymer is much higher than 300°C. Although at lower values of ω, the viscosity of Kraton G1651 is some fifty times greater than that of neat PPE, this viscosity difference becomes smaller with increasing ω. Since the viscosities of the Kraton G1651/PPE blends could not all be measured at higher frequencies by using the Rheometrics RMS 800 machine, we employed an

Table 2 Theoretically predicted values of the order–disorder transition temperature (T_r) of the SBS block copolymer

	T_r (°C)	
Interaction energy density parameter (Λ) used	Helfand–Wasserman theory	Leibler theory
From equation (3)	378	410
From equation (4)	425	464

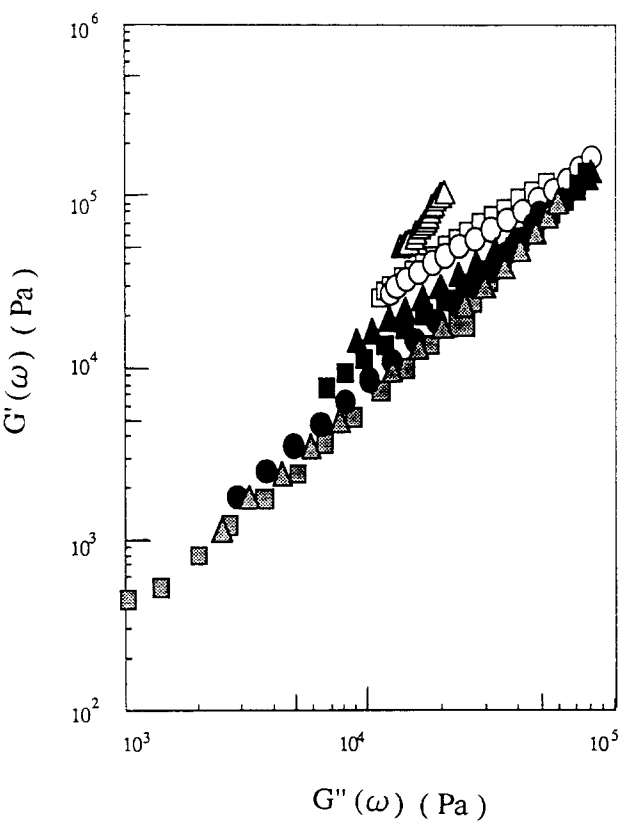

Figure 11 $\log G'(\omega)$ *versus* $\log G''(\omega)$ for the Kraton G1651/PPE blends at 300°C: △, Kraton G1651; ○, (P-1); □, (P-2); ▲, (P-3); ■, (P-4); ●, (P-5); △, (P-6); ⊠, PPE. The compositions of the blends are given in *Table 1*

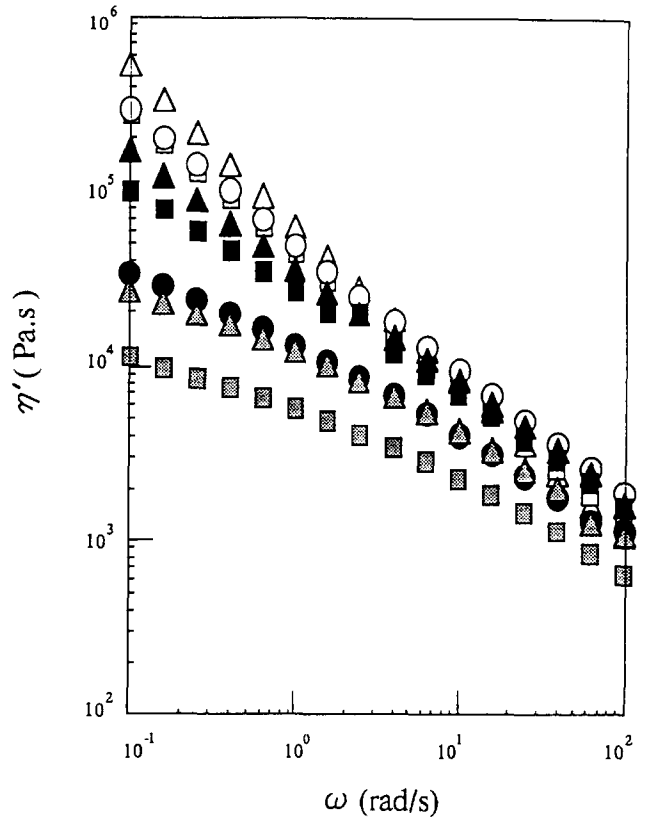

Figure 12 Plots of $\eta'(\omega)$ *versus* ω for the Kraton G1651/PPE blends at 300°C: △, Kraton G1651; ○, (P-1); □, (P-2); ▲, (P-3); ■, (P-4); ●, (P-5); ◬, (P-6); ▨, PPE. The compositions of the blends are given in *Table 1*

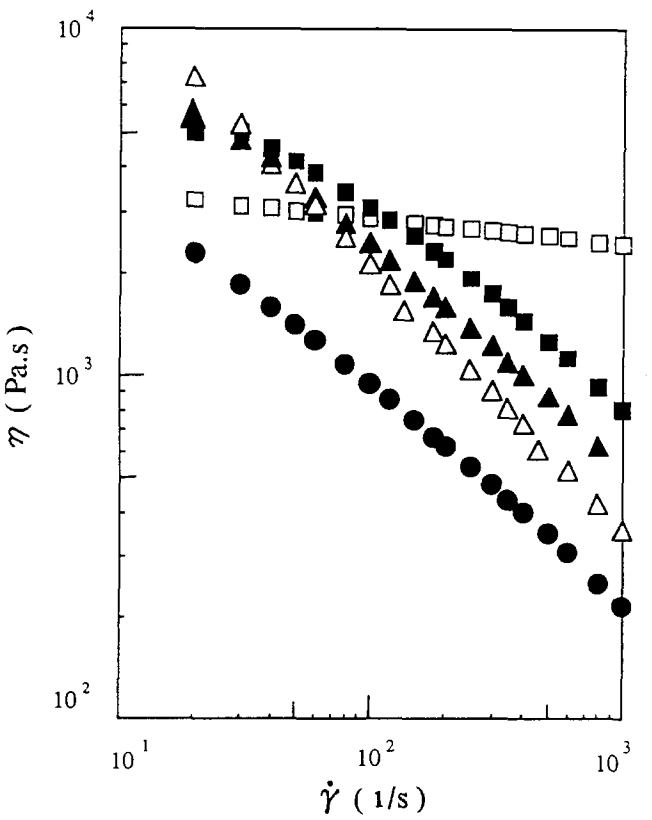

Figure 13 Viscosity *versus* shear rate measured by an Instron capillary rheometer for the Kraton G1651/PPE blends at 320°C: △, Kraton G1651; ●, (P-1); ▲, (P-3); ■, (P-5); □, PPE

Instron capillary rheometer for this work. *Figure 13* shows that at 320°C, the steady shear viscosity (η) of Kraton G1651 decreases dramatically with increasing shear rate ($\dot{\gamma}$), which indicates that the T_r of Kraton G1651 is even higher than 320°C. It can also be seen that at 320°C the viscosity of neat PPE changed very little with increasing $\dot{\gamma}$, and at higher values of $\dot{\gamma}$, the values of η obtained for samples (P-3) and (P-5) are even higher than those of Kraton G1651. It is of interest to note here that the viscosity of sample (P-1) is lower than that of neat PPE, even at $\dot{\gamma}=20\,s^{-1}$. This observation might be explained, in part, by the possibility that the principal direction of the lamellar microdomain structure found in sample (P-1) could be aligned to the flow direction when the shear rate is large.

Mechanical properties

The tensile and flexural strengths for Kraton G1651/PPE blends are given in *Figures 14a* and *b*, respectively. For Kraton G1651, the tensile and flexural strengths were too low to measure, while for the blends it can be seen from the figures that the tensile and flexural strengths both increase almost linearly with increasing amounts of PPE.

CONCLUSIONS

We have shown that the morphologies of various Kraton G1651/PPE blends prepared by an extrusion technique

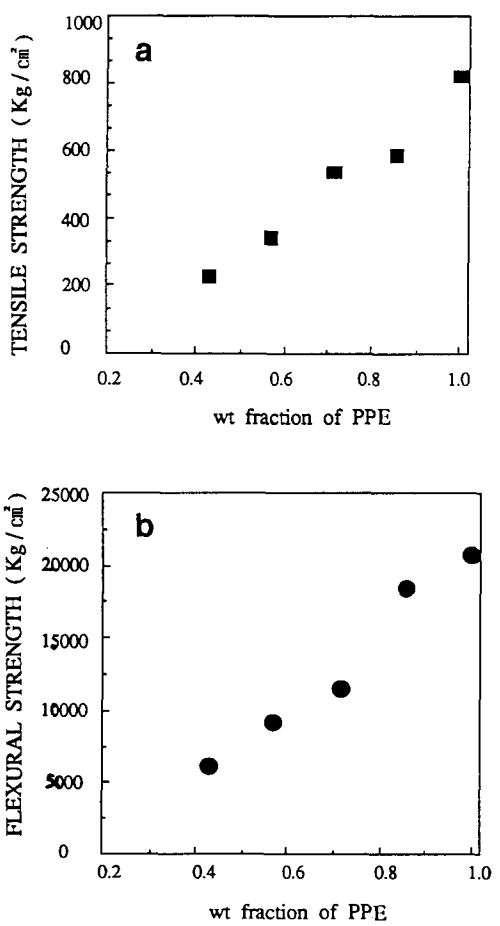

Figure 14 Changes in the mechanical properties as a function of the weight fraction of PPE in the Kraton G1651/PPE blends: a, tensile strength; b, flexural strength

were quite different from those of blends prepared by solution casting. In the former case, the effect of shear plays a very important role in the final morphology. Due to the relatively short contact time and high T_r of Kraton G1651, PPE homopolymer cannot be completely solubilized into the PS block in Kraton G1651 when the amount of homopolymer larger than 28.6 wt%. Sample (P-1), containing 14.3 wt% PPE appears transparent, and does not show any macrophase separation when examined by TEM. In addition, the microdomain structure in sample (P-1) consisted of lamellae. For sample (P-2), which contains 28.6 wt% PPE, *at least* part of the added PPE exists as macrophase-separated domains (observed by TEM), although a single T_g for the hard segment was detected by d.s.c. and d.m.t.a. Therefore, the existence of a single T_g with a broad transition range should not be construed as sufficient evidence that blends consisting of a block copolymer and a homopolymer are miscible (or compatible). More sophisticated techniques, such as solid-state n.m.r., should be employed to examine micro-heterogeneity, which cannot be detected by d.s.c. or d.m.t.a. techniques.

As the amount of PPE in the blends was increased, some portions of the former were solubilized into the PS domain in the block copolymer, but large portions of PPE existed in the macrophase-separated domains. In addition, dynamic shear modulus *versus* loss modulus plots were found to be very sensitive to the morphological variations in these homopolymer/block copolymer mixtures as a function of both the blend composition and temperature.

Since the Flory interaction parameter for a PEB/PPE pair is not yet available, we could not calculate the phase diagram for the Kraton G1651/PPE blends by using the equilibrium theories of Hong–Noolandi[25] and Whitmore–Noolandi[26]. Since all of the mixtures investigated in this study were not in an equilibrium state, we hope that the experimental results reported herein help towards the development of a theory for predicting the phase behaviour of homopolymer/block copolymer mixtures under shear flow. It should be mentioned that the compatibilizing effect of a block copolymer on immiscible homopolymer blends under shear-flow conditions has been very recently considered by Noolandi[58]. However, further theoretical work is required to interpret the experimental results that have been obtained for the phase behaviour of homopolymer/block copolymer mixtures prepared by extrusion techniques.

In future publications, we will present work on the morphology of blends prepared by various techniques, and compare the results with those reported here.

ACKNOWLEDGEMENTS

J. K. Kim thanks Dr J. K. Yeo, Senior Managing Director of the Research and Development Centre, Lucky Ltd, for his encouragement during this work and for allowing the work to be published. We wish to thank Professor J. W. Barlow for discussions of this work during the 34th IUPAC International Symposium. We also acknowledge the help of Dr H. Hasegawa and Professor T. Hashimoto in providing us with an unpublished transmission electron micrograph of Kraton G1652 and a copy of ref. 39.

REFERENCES

1 Inoue, T., Soen, T., Hashimoto, T. and Kawai, H. *Macromolecules* 1970, **3**, 87
2 Toy, L., Ninomi, M. and Shen, M. *J. Macromol. Sci. Phys.* 1975, **B11**, 281
3 Ninomi, M., Akovali, G. and Shen, M. *J. Macromol. Sci. Phys.* 1977, **B13**, 133
4 Cohen, R. E. and Ramos, A. R. *Macromolecules* 1979, **12**, 131
5 Bates, F. S., Berney, C. V. and Cohen, R. E. *Macromolecules* 1983, **16**, 1101
6 Zin, W. C. and Roe, R. J. *Macromolecules* 1984, **17**, 183
7 Roe, R. J. and Zin, W. C. *Macromolecules* 1984, **17**, 189
8 Nojima, S. and Roe, R. J. *Macromolecules* 1987, **20**, 1866
9 Tucker, P. S., Barlow, J. W. and Paul, D. R. *J. Appl. Polym. Sci.* 1987, **34**, 1817
10 Tucker, P. S., Barlow, J. W. and Paul, D. R. *Macromolecules* 1988, **21**, 1678
11 Tucker, P. S., Barlow, J. W. and Paul, D. R. *Macromolecules* 1988, **21**, 2794
12 Hashimoto, T., Kimishima, K. and Hasegawa, H. *Macromolecules* 1991, **24**, 5704
13 Han, C. D., Baek, D. M., Kim, J., Kimishima, K. and Hashimoto, T. *Macromolecules* 1992, **25**, 3052
14 Baek, D. M. and Han, C. D. *Macromolecules* 1992, **25**, 3706
15 Baek, D. M., Han, C. D. and Kim, J. K. *Polymer* 1992, **33**, 4821
16 Kim, J., Han, C. D. and Chu, S. G. *J. Polym. Sci., Polym. Phys. Edn* 1988, **26**, 677
17 Han, C. D., Kim, J., Baek, D. M. and Chu, S. G. *J. Polym. Sci., Polym. Phys. Edn* 1990, **28**, 315
18 Han, C. D., Kim, J., Kim, J. K. and Chu, S. G. *Macromolecules* 1989, **22**, 3443
19 Hashimoto, T., Tanaka, H. and Hasegawa, H. in 'Molecular Conformation and Dynamics of Macromolecules in Condensed Systems' (Ed. M. Nagasawa), Elsevier, Amsterdam, 1988, p. 257
20 Noolandi, J. and Hong, K. M. *Macromolecules* 1982, **15**, 382
21 Noolandi, J. *Polym. Eng. Sci.* 1984, **24**, 70
22 Vilgis, T. A. and Noolandi, J. *Macromolecules* 1990, **23**, 2341
23 Leibler, L. *Makromol. Chem. Makromol. Symp.* 1988, **16**, 1
24 Shull, K. K. and Kramer, E. J. *Macromolecules* 1990, **23**, 4769
25 Hong, K. M. and Noolandi, J. *Macromolecules* 1983, **16**, 1083
26 Whitmore, W. D. and Noolandi, J. *Macromolecules* 1985, **18**, 2486
27 Banaszak, M. *PhD Dissertation*, Memorial University of Newfoundland, St. John's, 1991
28 Leibler, L. and Benoit, H. *Polymer* 1981, **22**, 195
29 de la Cruz, M. O. and Sanchez, I. C. *Macromolecules* 1986, **19**, 2501
30 Mori, K., Tanaka, H. and Hashimoto, T. *Macromolecules* 1987, **20**, 381
31 Kang, C. K. and Zin, W. C. *Macromolecules* 1992, **25**, 3039
32 Utracki, L. A. 'Polymer Alloys and Blends', Oxford University Press, Oxford, 1989
33 Fox, T. G. *Bull. Am. Phys. Soc.* 1956, **1**, 126
34 Bohn, L. *Angew. Makromol. Chem.* 1971, **20**, 129
35 Bohn, L. *Adv. Chem. Ser.* 1975, **142**, 66
36 Moribitzer, L., Kranz, G. H. and Ott, K. H. *J. Appl. Polym. Sci.* 1976, **20**, 2691
37 Matsuo, M. *Polymer* 1968, **9**, 425
38 Folkes, M. L. and Keller, A. in 'Block and Graft Copolymers' (Eds J. J. Burke and V. Weiss), Syracuse University Press, Syracuse, NY, 1973, p. 87
39 Sakurai, S., Hasegawa, H. and Hashimoto, T. *Polym. Prepr. (Jpn)* 1990, **39**, 387
40 Gallot, R. B. *Adv. Polym. Sci.* 1978, **29**, 85
41 Ferry, J. D. 'Viscoelastic Properties of Polymers', 3rd Edn, Wiley, New York, 1980
42 Koberstein, J. T., Russell, T. P., Walsh, D. J. and Pottick, L. *Macromolecules* 1990, **23**, 877
43 Zin, W. C. and Roe, R. J. *Macromolecules* 1980, **13**, 1221
44 Lin, J. L. and Roe, R. J. *Macromolecules* 1987, **20**, 2168
45 Rounds, N. A. PhD Dissertation, University of Akron, 1971
46 Sakurai, S., Mori, K., Kimishima, K. and Hashimoto, T. *Macromolecules* 1992, **25**, 2679
47 Richardson, M. J. and Savill, N. G. *Polymer* 1977, **18**, 3
48 Rigby, D. and Roe, R. J. *Macromolecules* 1986, **19**, 721
49 Helfand, E. *Macromolecules* 1975, **8**, 552
50 Helfand, E. and Wasserman, Z. R. *Macromolecules* 1978, **11**, 960
51 Helfand, E. and Wasserman, Z. R. in 'Developments in Block Copolymers' (Ed. I. Goodman), Applied Science, London, 1982, Ch. 4, p. 99

52 Leibler, L. *Macromolecules* 1980, **13**, 1602
53 Sakurai, S., Hasegawa, H., Hashimoto, T. and Han, C. C. *Polym. Commun.* 1990, **31**, 99
54 Han, C. D., Kim, J. and Kim, J. K. *Macromolecules* 1989, **22**, 383
55 Gergen, W. P. *Kautschuk Gummi* 1984, **37**, 284
56 Kawamura, T., Yokoyama, K., Fujita, Y. and Toki, S. Proceedings of 7th Annual Meeting of the Polymer Processing Society, Hamilton, Canada, April 1991, p. 170
57 Han, C. D. and Kim, J. K. *Polymer* 1993, **34**, 2533
58 Noolandi, J. *Makromol. Chem. Rapid Commun.* 1991, **12**, 517